Characterization of Via Etching in CHF_3/CF_4 Magnetically Enhanced Reactive Ion Etching Using Neural Networks

Sung Ku Kwon, Kwang Ho Kwon, Byung Whan Kim, Jong Moon Park, Seong Wook Yoo, Kun Sik Park, Yoon Kyu Bae, and Bo Woo Kim

This study characterizes an oxide etching process in a magnetically enhanced reactive ion etching (MERIE) reactor with a CHF_3/CF_4 gas chemistry. We use a statistical 2^{4-1} experimental design plus one center point to characterize the relationships between the process factors and etch responses. The factors that we varied in the design include RF power, pressure, and gas composition, and the modeled etch responses were the etch rate, etch selectivity to TiN, and uniformity. The developed models produced 3D response plots.

Etching of SiO_2 mainly depends on F density and ion bombardment. SiO_2 etch selectivity to TiN sensitively depends on the F density in the plasma and the effects of ion bombardment. The process conditions for a high etch selectivity are a 0.3 to 0.5 CF_4 flow ratio and a –600 V to –650 V DC bias voltage according to the process pressure in our experiment. Etching uniformity was improved with an increase in the CF_4 flow ratio in the gas mixture, an increase in the source power, and a higher pressure.

Our characterization of via etching in a CHF_3/CF_4 MERIE using neural networks was successful, economical, and effective. The results provide highly valuable information about etching mechanisms and optimum etching conditions.

Manuscript received Nov. 22, 2001; revised Feb. 15, 2002.

Sung Ku Kwon (phone: +82 42 860 6205, e-mail: skkwon@etri.re.kr), Jong Moon Park (e-mail: jmpark@etri.re.kr), Seong Wook Yoo (e-mail: ysw@etri.re.kr), Kun Sik Park (e-mail: kunsik@etri.re.kr), Yoon Kyu Bae (e-mail: ykbae@etri.re.kr), and Bo Woo Kim (e-mail: bwkim@etri.re.kr) are with Basic Research Laboratory, ETRI, Daejeon, Korea.

Kwang Ho Kwon (e-mail: khkwon@hanseo.ac.kr) is with the Department of Electronic Engineering, Hanseo University, Seosan, Korea.

Byung Whan Kim (e-mail: kbwhan@sejong.ac.kr) is with the Department of Electronic Engineering, Sejong University, Korea.

I. INTRODUCTION

Plasma etching has gained widespread use in the manufacture of very large scale integrated circuits [1]. Its advantages include anisotropic pattern formation, high-fidelity pattern transfer, and processing at a relatively low temperature. As device dimensions in ultra large scale integration continue to shrink, plasma etching will become more essential in many critical fabrication processes, such as gate poly, contact & via, and metal etch processes [2]. At the same time, requirements for etching selectivity, line-width control, etching uniformity, and the etched profile have become more stringent and more difficult to meet [3]. In particular, sub-micron patterns and high aspect ratios (>10:1) have created unexpected problems in via etching for inter-metal connections. Accordingly, in order to obtain low via resistance and a wide process window, the uniformity and selectivity to the TiN of etched inter-metal dielectrics (IMD) films should be strictly controlled.

Optimizing a via-etch process is extremely difficult because of the complex relationships between the process factors and etch responses as well as some trade-offs between the responses. It is thus critical to develop computer simulation models to discover ways to form via holes in a cost-effective way. Historically, newly developed plasma models have used the first principles of physics involving continuity, momentum balance, and energy balance inside a high frequency, high intensity electric or magnetic field. Because the physical and chemical features of these processes are often not well understood, they are subject to many simplifying assumptions, which often result in significant discrepancies between model

predictions and actual measurements. As an alternative, some studies have adopted adaptive learning techniques which use neural networks combined with statistical experimental designs to understand the underlying etch mechanisms [4]-[7]. Neural net plasma models once demonstrated improved prediction over statistical response surface models in modeling plasma etch processes [8], [9].

In our investigation, neural networks modeled the characteristics of oxide film etched in $CHF_3/CF_4/Ar$ gas chemistry, and a magnetically enhanced reactive ion etcher (MERIE) performed the etching. We used a statistical experimental design to systematically characterize relationships between process factors and etch responses. The factors that were varied in the design include RF power, pressure, and CHF_3 and CF_4 flow rates. In addition to the conventional etch rate, we also modeled etch uniformity and selectivity to TiN.

II. EXPERIMENTAL APPARATUS AND DESIGN

1. Apparatus

Figure 1 depicts a schematic diagram of the MERIE system (P-5000MxP) we used for the oxide etching. With the upper plate grounded, the lower one is capacitively coupled to a 13.56 MHz RF power supply by a matching network. The magnetic field parallel to the lower electrode is generated by the electromagnetic coils mounted around the outside of the reactor chamber. During the etching, the substrate holder temperature was held at 20°C.

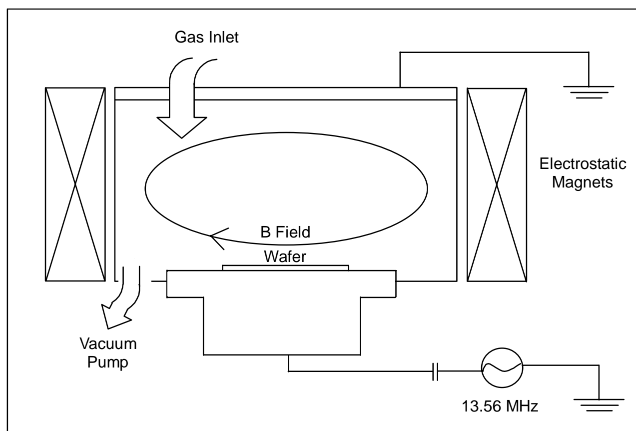

Fig. 1. Schematic diagram of the magnetically enhanced RIE system (P-5000MxP).

2. Experimental Design

To characterize the relationships between the process factors and etch characteristics, we used a statistical 2^{4-1} full factorial design [10] with one center point. The factors that were varied include RF power, pressure, CHF_3 and CF_4 flow rates. Table 1 gives the experimental ranges of the factors. Nine experiments were used to train the neural networks and the trained networks were tested in 8 additional experiments. Thus, a total of 17 experiments were performed to develop a predictive etch model.

3. Experiments

Test patterns were fabricated on (100) oriented Si substrates, which were doped with Boron (1–30 Ω-cm) and chemically cleaned for 600 seconds using a 4 H_2SO_4:1 H_2O_2 mixture solution at a temperature of 110°C. This was then followed by a de-ionized water rinse prior to plasma enhanced chemical vapor deposition (PECVD). Oxide films with a thickness of about 900 nm were prepared on the chemically pre-cleaned (100) silicon by the reaction of SiH_4 and N_2O in a plasma-enhanced CVD reactor at a substrate temperature of 400°C and reaction pressure of 3 Torr. Using a spin coater, the 1.02 µm thick photoresist-film was coated at an RPM of 4000 and subsequently soft-baked for 90 seconds at a temperature of 90°Con the hot plate in the track system (TEL Mark-Vz). A PR pattern with equal lines & spaces and holes was formed using an i-line Nikon stepper (NSR2205i11D). The developed samples were subsequently hard-baked at 120°C for 30 minutes in a convection oven.

The etching experiments were carried out in a MERIE reactor equipped with an optical emission spectrometer to analyze the active species in the gas phase. Table 1 gives the range and values of the main independent variables and constants for the MERIE etching process. A NanoSpec 3000 spectroscopic reflectometer measured the film's thickness. The etch rate data were extracted at the no-patterned region by dividing the etched film thickness by the etch time.

In-situ optical emission spectroscopy (OES), which was built into the system, performed the analysis of the gas mixtures. The emission light from the glow discharge of different feed

Table 1. Range and values of the main independent variables and constants for the MERIE etching process.

Parameter	Range	Units
CHF_3	20 – 80	sccm
CF_4	10 – 40	sccm
Pressure	50 – 200	mTorr
RF Power	300 – 800	Watts

gas mixtures was focused with a quartz lens and introduced into a monochromator. The OES apparatus for the experiments consisted of a photomultiplier tube and a conventional photo-counting system comprising a discriminator, a multi-channel scaler, and a personal computer. Optical emission measurements were made in the range of wavelengths between 200 and 800 nm with a resolution of 0.25 nm. During optical emission measurements, 90 sccm of Ar gas was introduced into the reaction chamber to provide a reference peak. The spectral positions for CF_2, F, H, and Ar were 321.4 nm, 731.3 nm, 656 nm, and 707.0 nm, respectively.

III. NEURAL NETWORKS

Among the various paradigms of artificial neural networks, we chose the back-propagation neural network (BPNN) [11] for this plasma modeling because of its proven high accuracy in learning nonlinear process data. A typical architecture of BPNN is exhibited in Fig. 2.

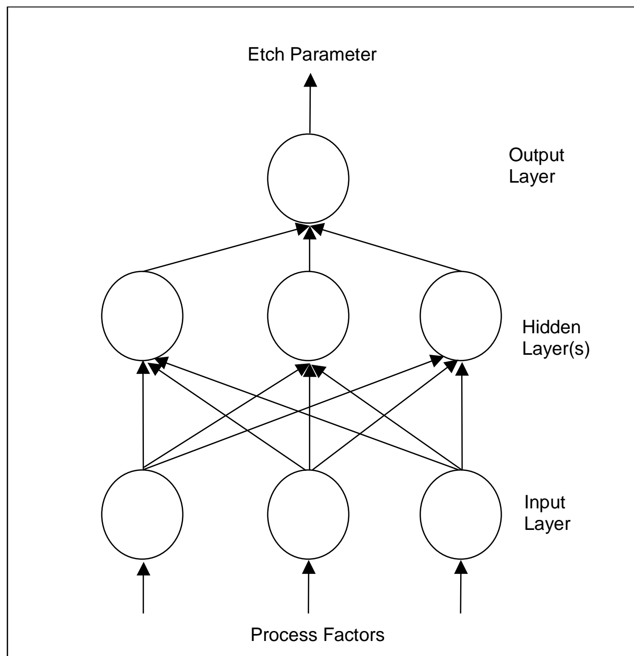

Fig. 2. A schematic diagram of a backpropagation neural network.

The BPNN consists of the following layers of neurons: input layer, hidden layer, and output layer. The input layer receives external information such as that represented by the three adjustable equipment parameters in Table 1. The output layer transmits the data and thus corresponds to the various plasma attributes (electron density, electron temperature, and plasma potential). In this study, the number of neurons in the output layer was set to unity since each attribute was modeled one by one. The BPNN also incorporates "hidden" layers of neurons that do not interact with the outside world, but assist in performing nonlinear feature extraction on the data provided by the input and output layers. The activation level (or firing strength) of a neuron was determined by a nonlinear sigmoid function denoted as

$$out_{i,k} = \frac{1}{1+e^{-\mathrm{int}_{i,k}}}, \tag{1}$$

where $\mathrm{int}_{i,k}$ and $out_{i,k}$ indicate the weighted input to the i-th neuron in the k-th layer and output from that neuron.

The BP algorithm by which the network is trained begins with a random set of weights (i.e., connection strengths between neurons). An input vector, which has been normalized to lie in the interval between –1 and 1, is then presented to the network, and the output is calculated using an initial weight matrix. Next, the calculated (or predicted) output is compared to the actually measured output, and the squared difference between the two determines the system error. The Euclidean distance in the weight space that the network attempts to minimize is the accumulated error (E) of all the input-output pairs, which is expressed as

$$E = 0.5\sum_{j=1}^{q}(d_j - out_j)^2, \tag{2}$$

where q is the number of output neurons, d_j is the desired output of the j-th neuron in the output layer, and out_j is the calculated output of that same neuron. In the BP algorithm, this error is minimized by *gradient descent* optimization, in which the weights are adjusted in the direction of decreasing the E in (2). A basic weight update scheme, commonly known as the generalized delta rule [11], is expressed as

$$W_{i,j,k}(m+1) = W_{i,j,k}(m) + \eta\Delta W_{i,j,k}(m), \tag{3}$$

where $W_{i,j,k}$ is the connection strength between the j-th neuron in the layer ($k-1$) and the i-th neuron in the layer k, and $\Delta W_{i,j,k}$ is the calculated change in the weight to minimize the E in (2) and defined as

$$\Delta W_{i,j,k} = -\frac{\partial E}{\partial W_{i,j,k}}. \tag{4}$$

The other terms, m and η, indicate the iteration number and an adjustable parameter called the "learning rate," respectively. By adjusting weighted connections recursively using the rule in (4) for all the units in the network, the accumulated E over all the input vectors is minimized.

IV. RESULTS AND DISCUSSION

1. Model Development

Using neural networks, we developed predictive etch models. Among many paradigms, we selected the backpropagation neural network (BPNN) because of its popularity in plasma-driven processes [4]-[8]. The BPNN was trained on the nine experiments obtained from a 2^{4-1} experiment and one center point. We tested the trained model on eight additional experiments. Although many training variables are typically involved [12], [13], in this study, we optimized only one hidden neuron variable under random initial weights. The number of hidden neurons was varied from 3 to 6 experimentally. In a previous study [13], multiple models of 200 were generated for a fixed number of hidden neurons to take into account randomness in the initial weight distribution. We selected only one model with a minimum prediction error out of 200 local minima and used this model to make various 3-D plots. We optimized 6 hidden neurons for the etch rate, 5 for etch uniformity, and 5 for selectivity to TiN. The prediction errors corresponding to the optimal hidden neurons were 149.8 Å/min for the etch rate, 0.807 for etch uniformity, and 26.30 for selectivity to TiN. Here, the prediction error was quantified with the root-mean squared error metric.

2. Etch Rate

Figure 3 plots the etch rates of oxide with various CF_4 and CHF_3 gas flow rates at a pressure of 125 mTorr and RF power of 550 W. This figure shows that etch rates of oxide films increase with an increasing CF_4 flow rate and a decreasing CHF_3 flow rate. In general, F radicals generated in the plasma react with oxide and form compounds of COF_2 and SiF_4, finally exerting the dominant influence on the etching of oxide films [14]-[16]. At the same time, the increase in the CHF_3 flow rate forms a compound of HF in the plasma, finally decreasing the density of F radicals in the plasma [13]. Therefore, the increase of the CF_4 flow rate and the decrease of the CHF_3 flow rate enhances the density of F radicals in the plasma, and thus increases the etch rates of the oxide films.

To obtain information on the reaction mechanism related to CF_4/CHF_3 gas composition, the active species generated as a function of gas composition in the plasma and etch residues on the etched SiO_2 surface were analyzed with an optical emission spectroscopy (OES) and x-ray photoelectron spectroscopy (XPS), respectively. XPS (ESCALAB 200R_VG Scientific) analyses were performed by collecting photoelectrons emitted from the sample surfaces with the characteristic kinematic energy of C1s and F1s, respectively at pass energies of 20 eV with an Al Kα x-ray source at take-off angles of 90°. Relative

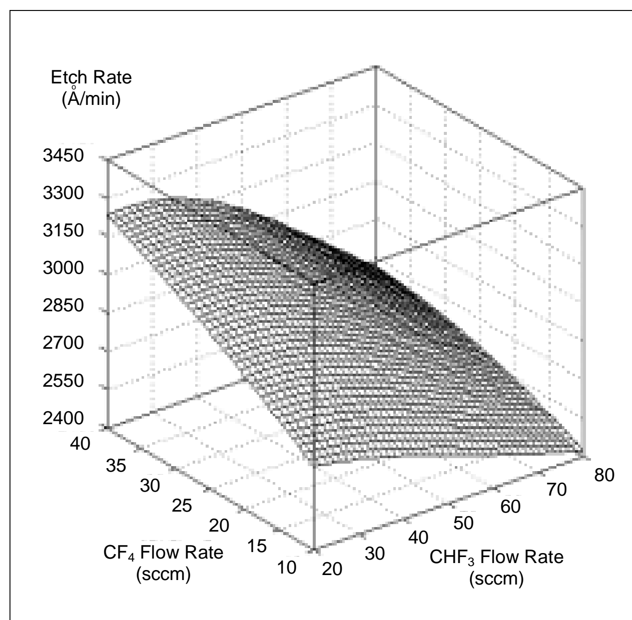

Fig. 3. Etch rates with various CF_4 and CHF_3 gas flow rates.

peak intensities for the C1s (290–295eV) and F1s (694eV) in the XPS analysis were normalized with respect to the highest relative intensity.

Figure 4(a) shows the variation of F, H, and CF_2 in the plasma as a function of the $CF_4/(CF_4+CHF_3)$ flow ratio with a source power of 550 W and pressure of 125 mTorr. In the regimes of I-II, while the emission intensity of F in the OES analysis continuously decreased with an increase of the CF_4 flow ratio, the maximal emission intensity of H and CF_2 species was obtained at a CF_4 flow ratio of 0.13. We assumed that the increase of H and CF_2 in regime I was induced by fast polymer decomposition with the increase of the CF_4 flow ratio.

In regime III, the emission intensity of F and CF_2 slowly increased, but the emission intensity of H did not increase because of the decrease of the CHF_3 flow ratio. We assumed that the F radical was intensively participating in the reaction of the polymer decomposition and SiO_2 etching with the increase of the CF_4 flow ratio in regime I. This is confirmed by the sharp decrease in the intensity of C1s and F1s on the surface of the etched samples (Fig. 4(b)) and the steep increase of the SiO_2 etch rate (Fig. 4(c)). H. Park et al. [17] reported that the 4 nm thick CF_X residue formed on a surface etched with CHF_3/C_2F_6 gas in reactive ion etching was easily removed by NF_3 plasma treatment. Therefore, with the increase of the CF_4 flow ratio, the decrease in the intensity of C1s on the surface of the etched samples (Fig. 4(b)) well agrees with H. Park's results. In regime II of Fig. 4(a), the fast decrease in the intensity of H was caused by the reaction with F for HF formation and dilution of CHF_3 in the gas mixture. CF_2 was generated not only by dissociation of CF_4 and CHF_3, but also

by the reaction of CF_3 with H. Thus, the intensity of CF_2 was proportional to the H intensity in regime I-II. The increase of F in regime III was caused by an increase of the CF_4 flow ratio and a decrease of the polymer deposition, while the increase of CF_2 in regime III was caused by an increase of the CF_4 flow ratio and a competitive reaction with the increased F on the SiO_2 surface. We speculated about the roles of F, H, and CF_X radicals to explain the etch phenomenon in each regime. The role of the F radical is etching of the polymer layer and SiO_2; the role of the H radical is scavenging the F radical by forming an HF compound [12], which is an ineffective species for SiO_2 etching, which inhibits surface adsorption of the F radical by competitive surface adsorption while enhancing the surface polymerization with co-adsorbed CF_X and CHF_X species.

From these results, in regime I, we inferred that etching of SiO_2 mainly occurred at the interface between the thick-polymer and SiO_2 by the diffusion of the active species and ion bombardment. Thus, the etch rate of the SiO_2 steeply increased with a decrease of the polymer thickness caused by an increase in the CF_4 flow ratio. In regime III, because of a thin polymer layer, the etch rate of the SiO_2 mainly occurred on the SiO_2 surface according to the F density. In regime II, the etching of the SiO_2 proceeded with little polymer deposition according to the density of the active species and ion bombardment.

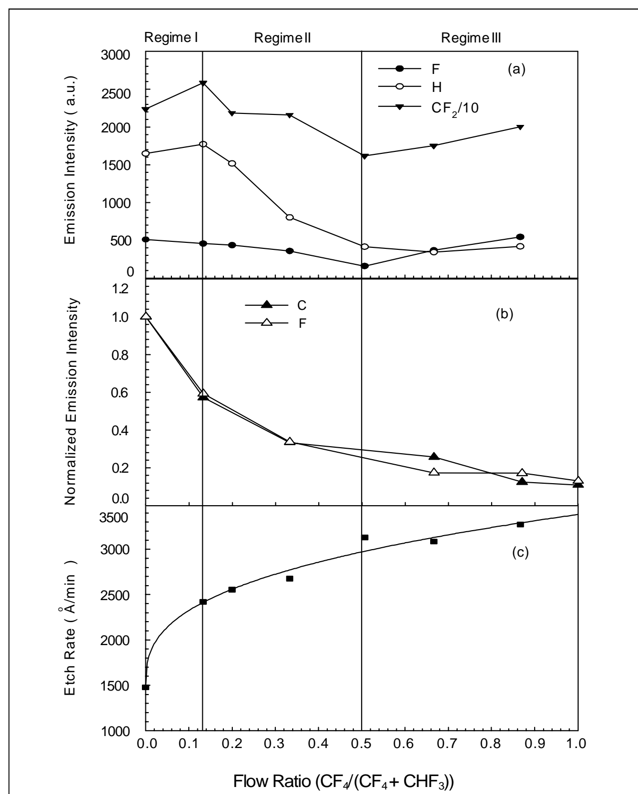

Fig. 4. (a) Optical emission intensity of F, H, CF_2 in plasma phase, (b) normalized emission intensity of C1s and F1s on the etched SiO_2 surface by XPS, (c) the blank etch rate of SiO_2 as a function of the CF_4 flow ratio in a $CF_4/(CF_4+CHF_3)$ gas mixture.

According to the gas composition of $CF_4/(CF_4+CHF_3)$, the etching mode of the oxide film converted from a thin polymer layer and an F species dominated chemical reaction at a high CF_4 ratio in the gas mixture to a thick polymer layer and an F species density dependent reaction at a low CF_4 ratio in the gas mixture through the transient region.

Figure 5 plots the etch rates of the oxide at various pressures and RF powers at a CF_4 flow rate of 50 sccm and CHF_3 of 25 sccm. Generally, etch rates depend on the chemical reactions by radicals and the physical effects by ion bombardment. Meanwhile, the effects of ion bombardment rely on ion densities and DC bias voltages.

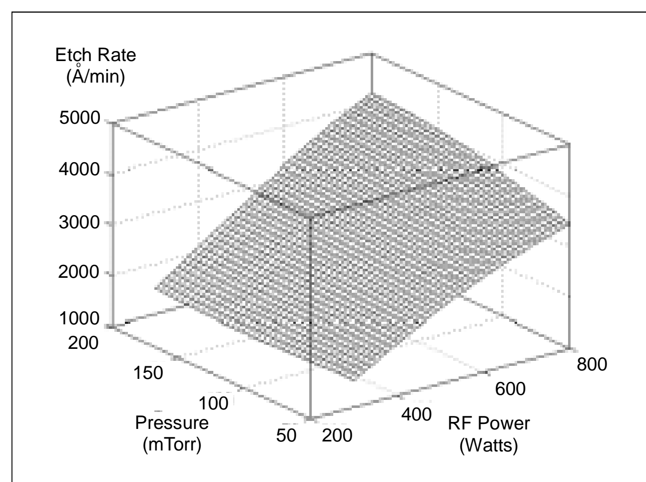

Fig. 5. Etch rates with various pressure and RF power.

Morgan found that an increase of pressure increases the densities of F radicals at a sufficient RF power, but on the other hand, decreases the DC bias voltage [18]. We actually found that the DC bias greatly decreased from –669 V to –528 V as the pressure increased from 50 mTorr to 200 mTorr at a 550 W RF power, a CF_4 flow rate of 50 sccm, and a CHF_3 flow rate of 25 sccm. In our results, the etch rate of SiO_2 slightly decreased with an increase of pressure at an RF power of 300 W because of the decreasing DC bias voltage. On the other hand, at an RF power of 800 W, although the DC bias voltage decreased with an increase of pressure, the ion bombardment energy for the etching reaction was still sufficiently high and the density of the active species was slightly increased. Thus, the etch rate of SiO_2 increased with an increase of pressure.

Meanwhile, Rummelhart and McClelland reported that an increase of the RF power increases the densities of the F radicals and the DC bias voltage together [11]. This shows that the chemical reactions by radicals and the physical effects by ion bombardment increase simultaneously. As a result, etch

rates increase sharply with an increase in RF power (Fig. 5). From this result, we concluded that RF power has a greater influence on etch rates of oxide films than pressure. In Figure 5, we can also see that etch rates at a pressure of 200 mTorr increase more sharply than those at 50 mTorr. This difference seems to be due to the differences of density of the active species at each pressure. In other words, while etch rates sharply increase with RF power at a pressure of 200 mTorr because of the sufficient supply of active etching species, etch rates increase more slowly at a chamber pressure of 50 mTorr because of the deficient supply of active etching species.

3. Etch Selectivity

Figure 6 compares the etching selectivity of SiO_2 films and TiN films at various RF powers and CF_4 gas flow rates with constant Ar and CHF_3 gas flow rates of 90 and 50 sccm, respectively. Prior to this work, we examined the etching rate of TiN films with various CF_4 gas flow rates and found an increase in the TiN etch rate with an increase in the CF_4 gas flow rate. This result is well in accord with Choi et al. [19]. Their report described that TiF_X (x = 3, 4) was an etching by-product and the formation of TiF_X (x = 3, 4) depended on the F radical density. This explanation indicates that the etching rate of TiN increases with an increase in the CF_4 gas flow rate. At the same time, they also found that the etch rate of oxide films increased with an increase in the CF_4 gas flow rate.

Figure 6 shows an increase in the selectivity with an increase in the CF_4 gas flow rate at 800 W RF power. This means that the etching rate of oxide films increases more sharply than that of TiN films within the experimental range of this study. This difference seemed to be due to the volatility of etching by-products, such as SiF_4 and TiF_X. While SiF_4, an etching by-product of oxide films, has a high volatility (a vapor pressure of

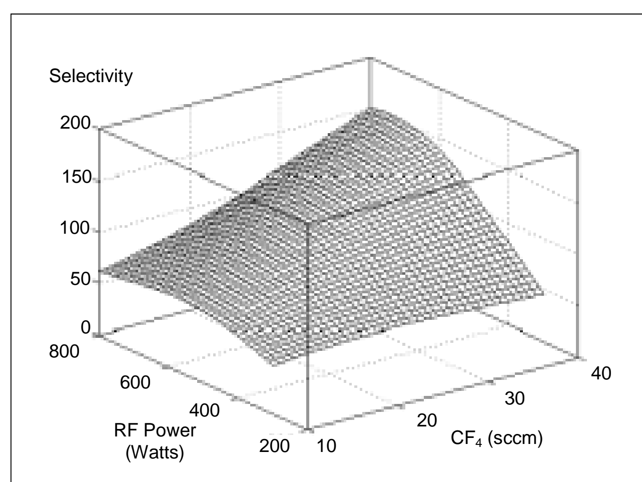

Fig. 6. Etching selectivity of SiO_2/TiN films with various RF power and CF_4 gas flow rates.

1 mmHg @ – 144°C), the boiling points of TiF_3 and TiF_4, etching by-products of TiN films, are 1400°C and 248°C, respectively. This means that the vaporization of TiF_X is more difficult to achieve than that of SiF_4.

At an RF power of 300 W, the etch selectivity of SiO_2/TiN scarcely varied with an increase of the CF_4 ratio in the gas mixture. This reveals that at a relatively smaller RF power, the etch rate of SiO_2 and TiN film is not largely affected by an increase in F intensity.

At an RF power of 800 W, the etch selectivity of SiO_2/TiN increased with an increase in the CF_4 flow rate ratio in the gas mixture. At a high RF power, the etch rate of SiO_2 sharply increased with an increase in the CF_4 gas flow ratio, because SiO_2 film has a self-containing O atom, which makes it less sensitive to surface polymerization than TiN film, and high volatility of etching by-products. With a higher CF_4 flow-rate ratio at a high source power, the difference in the etching reaction was only in the volatility of the etching by-products. Thus, at a CF_4 gas flow ratio higher than 0.5, the etch selectivity of SiO_2/TiN decreased, although this is not seen in Fig. 6. At a CF_4 flow rate of 10 sccm, the etch selectivity of SiO_2/TiN slowly increased at an RF power under 500 W and then remained constant at an RF power over 500 W. In this low power regime, the slow increase of SiO_2 etch selectivity to TiN was caused by the self-containing O atom and high volatility of SiF_4 compared to TiF_X (x=3, 4). At a high power regime, both SiO_2 and TiN were etched by ion bombardment and suffered a low etch rate because of the intense surface polymerization and low density of F species. Thus, the etch selectivity of SiO_2/TiN does not increase at the range of a high RF power and a high CHF_3 flow rate.

At a CF_4 flow rate of 40 sccm, the etch selectivity of SiO_2/TiN increased at an RF power under 630 W and remained constant at an RF power over 630 W. At a low CHF_3 gas ratio and 300–630 W RF power regimes, carbon-containing polymer deposition did not actively occur on either film surface. Thus, the increase in the etch rate of SiO_2 film that has a self-containing O atom and high volatility of etching by-products is faster than that of TiN film. However, the rate of increase in the TiN etch rate is steep at an RF power over 630 W because the energy of the ion bombardment is sufficient for the removal of the etch by-products. Thus, the increasing rate of the etch selectivity slowed down and finally decreased. The maximal etch-selectivity was obtained at the condition of 600–700 W RF power and a high CF_4 flow ratio of 0.5 in the gas mixture. Thus, the SiO_2 etch selectivity to TiN sensitively depends on the F density in the plasma and on the effects of ion bombardment.

These results reveal that etching of TiN suffered from surface polymerization and low volatility of etch by-products such as

TiF_3 and TiF_4. On the other hand, etch of SiO_2 depends on ion bombardment and F dominated etching rather than surface polymerization because the oxygen content of SiO_2 film partly participates in the polymer removal reaction.

Figure 7 plots the etching selectivity of TiN films at various pressures and RF powers. This figure shows that the selectivity increases with an increase in chamber pressure and RF power. To understand this, we examined the etching selectivity of SiO_2/TiN as a function of DC bias voltage with a fixed pressure. In this case, the RF power controlled the DC bias voltage. Figure 8 reveals that a maximal etch selectivity of 130 was obtained at a DC bias voltage of –617 V. Above –617 V, the etch selectivity of SiO_2/TiN decreased sharply. The etch rate of SiO_2 sharply increased with an increase in the DC bias voltage, and then the rate of increase of the SiO_2 etch rate slowed down with an insufficient supply of active species. However, the etch rate of TiN was not much influenced by the increase of the DC bias voltage until –617 V because of the low volatility of the etch by-products. Above –617 V, the etch rate of TiN sharply increased, and the etch selectivity of SiO_2/TiN also sharply decreased.

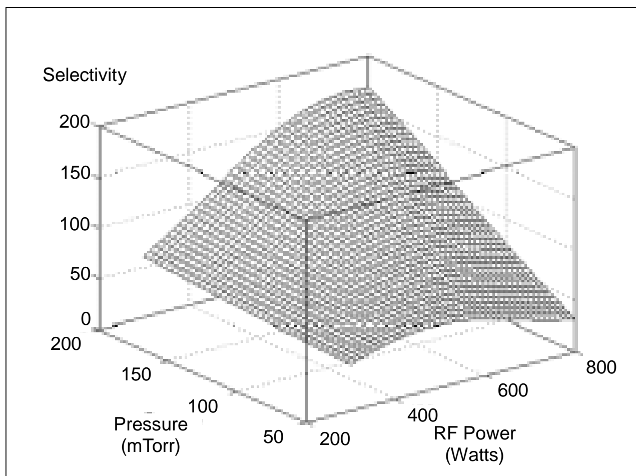

Fig. 7. Etching selectivity of TiN films at various pressures and RF powers.

According to H. Singh et al. [20], with an increase in pressure, the electron temperature, which was a major factor for dissociation of reaction gas, sharply decreased and resulted in an abundance of CF_X in the CF_4 plasma. In this way, the density behavior of F was explained by the electron temperature, which depends on the RF power and pressure. Therefore, with an increase of pressure, the polymerization reaction of both the gas phase and surface actively occurred in spite of a continued high DC bias voltage, an inhibited surface reaction between TiN and F radicals, and the removal of TiN etching by-products.

However, SiO_2 etch depends more on DC bias and F density

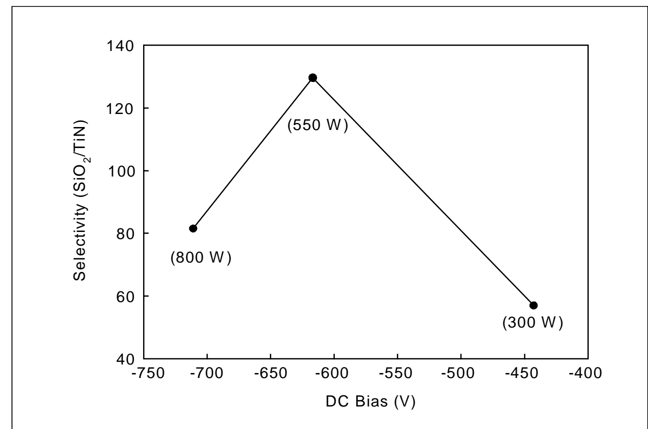

Fig. 8. Etch selectivity of (SiO_2/TiN) as a function of DC Bias voltage. (Pressure = 125 mTorr, M_Field=50 Gauss, CHF_3/CF_4/Ar=50/25/90 sccm).

with a high volatility of SiF_4 than on CF_X abundance; this results in high etch selectivity with an increase of pressure at a relatively high DC bias voltage.

Our investigation revealed a reduction in the TiN etch rate with an increase in pressure. With an increase in the chamber pressure, we also found a decrease in the DC bias voltage. Actually, the DC bias greatly decreased from –669 V to –528 V as the pressure increased from 50 mTorr to 200 mTorr at a 550 W RF power and 50 and 25 sccm for CHF_3/CF_4. The etch rate of TiN sharply increased at the higher values of –600 V DC bias voltage. As opposed to this, the etch rate of SiO_2 sharply increased with an increase in chamber pressure within a DC bias voltage range of –500 V to –700 V.

4. Etch Uniformity

Figure 9 plots the etch uniformity with CF_4 and CHF_3 flow

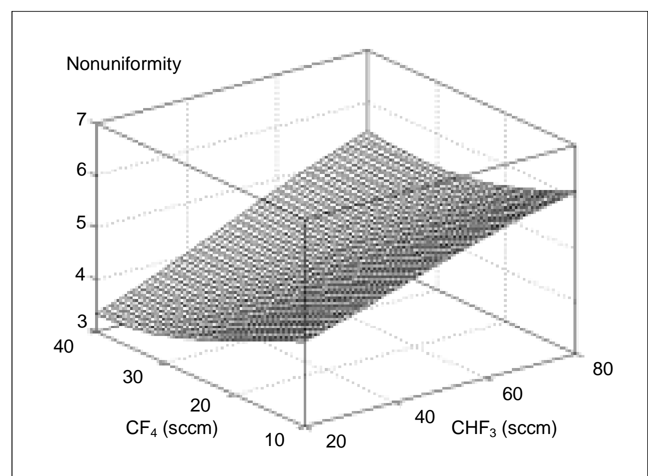

Fig. 9. Etch uniformity with CF_4 and CHF_3 flow rates.

rates. This figure indicates that the etch uniformity is enhanced with an increase in the CF_4 flow rate and a decrease in the CHF_3 flow rate. In general, the uniformity becomes worse when there is an increase in the thickness of a polymer layer which is largely influenced by CF_X (x<3) species. At the same time, CF_X (x<3) species are reduced with an increase in the CF_4 flow rate and a decrease in the CHF_3 flow rate. As a result, the etch uniformity is improved with an increase in the CF_4 flow rate and a decrease in the CHF_3 flow rate.

Figure 10 plots the etching uniformity at various pressures and RF powers. This figure shows that uniformity is improved with an increase in RF power and pressure.

The improvement of the uniformity with an increase in pressure can be inferred from the uniform distributions of the etching species in the chamber. At the same time, the uniformity improvement with an increase in RF power agrees with the report published by Holland et al. [21]. Holland reported that the formation of a polymer layer on the etching surface was closely related to the effect of ion bombardment, that is, the increase in RF power brings about an increase in DC bias voltage and then reduces the polymer thickness on the etching surface, thus, finally improving the uniformity. We can conclude that etching uniformity is closely related to surface polymerization, DC bias, and the density of the active species in the plasma.

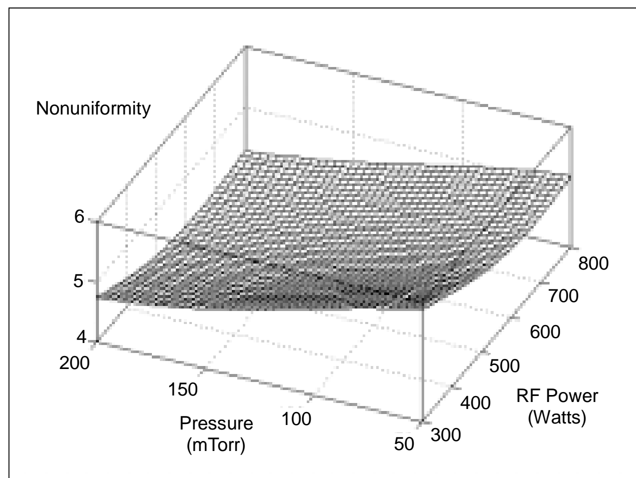

Fig. 10. Etching uniformity with various pressures and RF powers.

V. CONCLUSIONS

Our study characterized an oxide etch process in a magnetically enhanced reactive ion etching (MERIE) reactor with a CHF_3/CF_4 gas chemistry.

We characterized the relationships between process factors and etch responses with a statistical 2^{4-1} experimental design plus one center point. We varied the following factors in the design: RF power, pressure, and gas composition. The modeled etch responses were etch rate, etch selectivity to TiN, and uniformity.

Etching of SiO_2 mainly depends on F density and ion bombardment. The F density and DC bias voltages are major factors for TiN etch because the main role of these factors is the decomposition of polymers generated on the TiN surface and gasification of etch byproducts, such as TiF_3 or TiF_4, with high boiling temperature. We propose that the process condition for a high selectivity is a 0.3 to 0.5 CF_4 flow ratio and a –600 V to –650 V DC bias voltage according to the pressure.

The etching uniformity was improved with an increasing CF_4 flow ratio, increasing source power, and increasing pressure according to the pressure.

Our characterization of via etching in a CHF_3/CF_4 MERIE using neural networks was successful, economical, and effective. It provides highly valuable information about etching mechanisms and optimum etching conditions.

ACKNOWLEDGEMENT

The authors thank Y. S. Yoon, B. W. Lim, B. T. Lee, D. S. Sin, K. Y. Kim, B. M. Park for their help and fruitful discussions and assistance, and the K. MAC staff for the analysis of the etched samples.

REFERENCES

[1] R.J. Schutz, *VLSI Technology*, 2nd ed., edited by S.M. Sze, McGraw-Hill, New York, 1988.

[2] K. Baek, Y. Yoon, J. Park, K. Kwon, C. Kim, and K. Nam, “Corrosion at the Grain Boundary and a Fluorine-Related Passivation Layer on Etched Al-Cu (1%) Alloy Surfaces,” *ETRI J.*, vol. 21, no. 3, 1999, p.16.

[3] J.M. Cook and K.G. Donohoe, “Etching Issues at 0.35㎛ and below,” *Solid State Technol.*, vol. 34, 1991, p.119.

[4] B. Kim and G.S. May, “Reactive Ion Etch Modeling Using Neural Networks and Simulated Annealing,” *IEEE Trans. Comp. Pack. Manufact. Technol., Part C*, vol. 19, 1996, p. 3.

[5] B. Kim, K.H. Kwon, and S.H. Park, “Characterizing Metal-Masked Silica Etch Process in a CHF_3/CF_4 Inductively Coupled Plasma,” *J. Vac. Sci. Technol.*, vol. A 17, 1999, p. 2593.

[6] B. Kim, J. Sun, C. Choi, D. Lee, and Y. Seol, “Use of Neural Networks to Model Low-Temperature Tungsten Etch Characteristics in High Density SF_6 Plasma,” *J. Vac. Sci. Technol.*, vol. A18, 2000, p.417.

[7] C.D. Himmel and G.S. May, “Advantages of Plasma Etch Modeling Using Neural Networks over Statistical Techniques,” *IEEE Trans. Semicond. Manufact.*, vol. 6, 1993, p.103.

[8] B. Kim and G.T. Park, “Modeling Plasma Equipment Using Neural Networks,” *IEEE Trans Plasma Sci.*, vol. 29, 2001, p. 8.

[9] S.H. Oh and S.Y. Lee, “An Adaptive Learning Rate with Limited

Error Signals for Training of Multilayer Perceptrons," *ETRI J.*, vol. 22, no. 4, 2000, p. 40.
[10] D.C. Mongomery, *Design and Analysis of Experiments*, John Wiley & Sons, 1991.
[11] D.E. Rummelhart and J.L. McClelland, *Parallel Distributed Processing*, Cambridge, M.I.T. Press, 1986.
[12] B. Kim and G.S. May, "An Optimal Neural Network Process Model for Plasma Etching," *IEEE Trans. Semicond. Manufact.*, vol. 7, 1994, p.12.
[13] B. Kim and S. Park, "An Optimal Neural Network Plasma Model: a Case study," *Chemometr. Intell. Lab. Syst.*, vol. 56, 2001, p. 39.
[14] R. d'Agostino, F. Cramarossa, S.D. Benedictis, and G. Ferraro, "Spectroscopic Diagnostics of CF_4-O_2 Plasmas During Si and SiO_2 Etching Processes," *J. Applied Physics*, vol. 52, 1981, p. 1259.
[15] D.L. Flamm, C.J. Mogab, and E.R. Sklaver, "Reaction of Fluorine Atoms with SiO_2," *J. Applied Physics*, vol. 50, 1979, p. 6211.
[16] S. Kwon, K. Kim, C. Nam, and S. Woo, "Effect of CO and CO_2 Addition to the CF_4/O_2 Gas System on the Etching of a Low-Pressure Chemical Vapor Deposition Tungsten Film," *J. Vac. Sci. Technol.*, vol. B13, 1995, p.914.
[17] H. Park, K. Kwon, S. Lee, B. Koak, S. Nahm, H. Lee, K. Cho, O. Kwon, and Y. Kang, "A Study on Modified Silicon Surface after CHF_3/C_2F_6 Reactive Ion Etching," *ETRI J.*, vol. 16, no. 1, 1994, p.45.
[18] R.A. Morgan, *Plasma Etching in Semiconductor Fabrication*, Elsevier Science Publishing Company, 27, 1985.
[19] C.J. Choi, Y.S. Seol, and K.H. Baik, "TiN Etching and Its Effects on Tungsten Etching in SF_6/Ar Helicon Plasma," *Jpn. J. Applied Physics*, vol. 37, pt. 1, no. 3A, 1998, p.801.
[20] H. Singh, J.W. Coburn, and D.B. Graves, "Measurements of Neutral and Ion Composition, Neutral Temperature, and Electron Energy Distribution Function in a CF_4 Inductively Coupled Plasma," *J. Vac. Sci. Technol.*, vol. A 19, no. 3, 2001, p. 718.
[21] L. Holland, L. Laurenson, R.E. Hurley, and K. Williams, "The Behavior of Perfluoropolyether and Other Vacuum Fluids under Ion and Electron Bombardment," *Nuclear Instruments and Methods*, vol. 111, 1973, p.555.

Sung Ku Kwon was born in Kyungnam, Korea in 1965. He received his BS degree in chemical engineering from Yonsei University, Seoul, in 1988 and the MS and PhD degrees in chemical engineering from the Korea Advanced Institute of Science and Technology in 1991 and 2000, respectively. From 1992 to 1995, he was with Hyundai Electronics and developed process technology for DRAM. Since 2000, he has been a Senior Member of Research Staff at Electronics and Telecommunications Research Institute. His research is in the field of semiconductor processing. His current research interests include plasma processing and thin film processing for CMOS and nano-device.

Kwang Ho Kwon received his BS degree in electrical engineering from Korea University, Seoul, Korea, in 1985, and MS and PhD degrees in electrical engineering from Korea University, Seoul, Korea, in 1987 and 1993. Since 1987, he has been with ETRI, where he has been involved in the research and development of silicon semiconductor processing and plasma etching. He is currently an Assistant Professor in the Electrironic Engineering Department of Hanseo University, Chungnam, Korea.

Byung Whan Kim was born in Chungbuk, Korea in 1962. He received BS and MS degrees from Korea University in 1985 and 1987, and PhD degree from the Georgia Institute of Technology in 1995. From 1996 to 1998, he was with Hyundai Electronics and developed plasma equipment and process technology. From 1999 to 2001, he was a Faculty Member at Chunnam National University. Since 2001, he has been with the Department of Electronic Engineering of Sejong University. His research interests include neurofuzzy modeling and optimization of plasma processes, monitoring, control and diagnosis.

Jong Moon Park was born in 1959. He received BS and MS degrees in electronic engineering from Chonbuk National University in 1982 and 1991. He joined ETRI in 1985. His research field includes semiconductor processing of application specific integrated circuits. His current interests are CMOS device and lithography technologies.

Seong Wook Yoo was born in Pohang, Korea in 1969. He received BS and MS degrees in inorganic materials engineering from Kyungpook National University, Taegu, in 1991 and 1994. From 1994 to 1998, he worked at the LG Semicon Co., Ltd., Gumi, Korea, where he was engaged in the research and development of CMOS process technology. In 1998, he joined ETRI, Daejeon, Korea, where he works on semiconductor processing and device technology. His research interests include advanced semiconductor technology especially in the fields of the thin film characteristics and multi-level metallization processes.

Kun Sik Park was born in Chungdo, Korea in 1967. He received BS and MS degrees in material science from Korea Advanced Institute of Science and Technology (KAIST) in 1991 and 1996. From 1996 to 2000, he worked at the LG Semicon Co., Ltd., Chungju, Korea where he was engaged in the research and development of 256M DRAM device technology. Since 2000, he has been working in Basic Research Laboratory of ETRI, Daejeon, Korea, where he works on the research and development of CMOS processing and device technology.

Yoon Kyu Bae was born in Kyungbuk, Korea in 1955. He received his BS degree in chemical engineering from Hanbat University, Daejeon. Since 1980, he has been with ETRI as a Principal Member of Technical Staff in Basic Research Laboratory. His research interests include CMOS process technology and process utility.

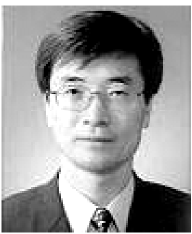

Bo Woo Kim was born in Pusan, Korea in 1952. He received BS and MS degrees in physics from Pusan National University in 1975 and 1978. He joined Samsung Semiconductor Inc. from 1978 to 1981 as Research Engineer, and the Department of Electronic Engineering at the University of Tokyo from 1986 to 1987 as Foreigner Researcher. Since 1981, he has been with ETRI as a Principal Member of the Engineering Staff in Basic Research Laboratory. His research interests include silicon based devices, processes, and nanotechnology.